Bulletin of Geosciences, Vol. 79, No. 3, 133–145, 2004
© Czech Geological Survey, ISSN 1214-1119

Contact metamorphism of Silurian black shales by a basalt sill: geological evidence and thermal modeling in the Barrandian Basin

Václav Suchý [1] – Jan Šafanda [2] – Ivana Sýkorová [3] – Michal Stejskal [4] – Vladimír Machovič [3, 4] – Karel Melka [5]*

[1] Varis RD, a. s., Na výšině 11/1474, 143 00 Praha 4, Czech Republic. E-mail: sediment@quick.cz
[2] Academy of Sciences of the Czech Republic, Geophysical Institute, Boční II/1401, 141 31 Praha 4, Czech Republic. E-mail: jsa@ig.cas.cz
[3] Academy of Sciences of the Czech Republic, Institute of Rock Structure and Mechanics, V Holešovičkách 41, 182 09 Praha 8, Czech Republic. E-mail: sykorova@irsm.cas.cz, vladimir.machovic@vscht.cz
[4] Institute of Chemical Technology, Technická 5, 166 28 Praha, Czech Republic. E-mail: michal.stejskal@vscht.cz
[5]Academy of Sciences of the Czech Republic, Institute of Geology, Rozvojová 135, 165 00 Praha 6, Czech Republic. E-mail: melka@gli.cas.cz
*corresponding author

Abstract. Organic-rich shales of the Liteň Formation (Silurian) were intruded by a series of several-meter thick doleritic basalt sills soon after their deposition. The effect of rapid thermal stress on organic and mineral diagenesis of shales around a representative 4 m thick sill has been studied using optical microscopy, Fourier-Transform infrared (FT-IR) and micro-Raman spectroscopy of dispersed graptolite particles, gas chromatography-mass spectrometry (GC-MS) of organic extracts, and X-ray diffraction (XRD) of the clay fraction.

Our data suggest that the sills have only had a local effect on the thermal maturity of the adjacent sediments. Graptolite reflectance values (3.0–3.6% R_{max}) and bireflectance (up to 3.1%) higher than the regional diagenetic background (~1.8 R_{max}) were found to be restricted to the narrow zone immediately adjacent to the igneous contacts, with detectable alteration starting to take effect at about 70 to 80% of sill thickness. Based on recent empirical correlations, these values may indicate contact-metamorphic temperatures between 320–420 °C. The optical properties of graptolite fragments within the contact aureole correlate closely with the chemical and structural transformation as expressed by FT-IR and Raman spectroscopy data. The graptolite periderm undergoes systematic depletion of aliphatic-containing groups toward the igneous contacts, and transforms into a condensed aromatic residuum of an increased crystalline ordering, similar to high-rank coal or kerogen. Extractable organic matter within the immediate contact zone is strongly depleted, but appreciably higher concentrations were obtained at a distance of 1.2 m below the intrusion. This suggests that the organic matter along the contact was gasified during the igneous event, and the expelled volatiles condensed in "micro-reservoirs" a certain distance from the sill.

In contrast to the organic matter, clay minerals from the contact aureole reveal a lower degree of thermal metamorphism. The values of illite crystallinity (IC; up to 0.44° Δ2θ) and chlorite crystallinity (ChC; 0.30–0.34° Δ2θ) recorded in a narrow contact zone imply only minor elevation above the regional diagenetic background (IC ~ 0.60–0.70° Δ2θ), and broadly evidence paleotemperatures in the range of 170–300 °C. The apparent discrepancy between the degree of thermal transformation of the organic matter and the clay minerals can be ascribed to the greater sensitivity of organic materials to geologically short metamorphic heating.

The results from computer thermal modeling of the sill do not match the empirical geological thermometers, as the model predicts substantially higher temperatures and wider contact zones. A reasonable fit between the two requires water-saturated magma that has cooled to about 600–700 °C. Given these preconditions, the modeling would predict maximum temperatures in the range 380–440 °C and contact aureoles exceeding 1–2 times the thickness of the sill. The thermal perturbation caused by the intrusion was short-lived and largely decayed into the diagenetic background within weeks to months after the emplacement.

Key words: contact metamorphism, basalt sill, black shale, graptolite reflectance, illite and chlorite crystallinity, thermal modeling, Barrandian, Silurian

Introduction

The extent to which organic matter and clay minerals are affected by igneous intrusions has been the subject of many petrological and geochemical studies (see Bostick and Clayton 1986, Robert 1988 for a review). Most of the work has shown that when an igneous body intrudes a sequence of sediments, the effect of thermal stress can be evident at distances from the contacts up to twice the thickness of the intrusion itself (Dow 1977). Several studies, however, have documented substantially thinner alteration zones (≤ 50% of the intrusion thickness), the effects of which were ascribed to varying thermal conductivities, rates of heat transfer, volumes of pore water, and the maturation level of the organic matter at the time when magma intruded the sediment (Saxby and Stephenson 1987, Raymond and Murchison 1988, Krynauw et al. 1994, and many others).

The present article reports another example of unusually thin contact aureoles developed around basalt sills that penetrated a Silurian black shale sequence in the Barrandian Lower Paleozoic basin. Some previous works in the area, though largely devoted to more general problems, have already mentioned elevated levels of organic maturity around some Barrandian basaltic sills (Malán 1980, Hrabal 1989, Kříbek 1989, Suchý et al. 1997). Here we discuss further empirical and computational evidence indicating that the limited contact aureoles were probably due to the high water content of the intruded shales, which seem to have still been soft and water-saturated during the intrusive event. In order to provide detailed insight into the mechanism of the heating effects, we investigated the organic and clayey matter within the enclosing sediments using several analytical techniques, including optical microscopy, FT-IR and micro-Raman spectroscopy of dispersed organic particles, and GC-MS of organic rock extracts. These tools provide organic-geochemical data that can be interpreted in terms of the paleothermal history of the organic matter (Tissot and Welte 1984, Robert 1988, Bustin et al. 1989,

Jehlička and Beny 1999). We also examined the degree of recrystallization of illite and chlorite, which gives useful, though less decisive, information on paleotemperatures around the intrusions (see Merriman and Frey 1999 for a review). Maturity parameters and paleothermal data derived from both organic and mineral constituents are compared to a computer-generated thermal model of the intrusion to assess how the empirical geological evidence corresponds to theoretical calculations.

Geological setting and samples

The Barrandian Basin of the central Czech Republic (Fig. 1) is an unmetamorphosed, structurally simple sedimentary sequence. The basin, which is about 90 km long and 25 km wide, was formed during the Ordovician as a narrow rift depression (Havlíček 1981). The depression was filled with more than 3500 m of marine siliciclastics and carbonates that gradually accumulated until the Middle Devonian (Chlupáč et al. 1998). During the Early Silurian, synsedimentary faults and associated submarine volcanoes created a complex topography within the basin, with volcanic seamounts fringed by shallow-water carbonate facies. Fine-grained, often graptolite-rich pelitic facies were deposited in a deeper-water basinal setting at depths between 150–200 m (Štorch and Pašava 1989). A number of additional basalt intrusions penetrated the Silurian and Ordovician sequences toward the end of the Silurian (Fiala 1970). These intrusions were emplaced below the seafloor at depths between 100–200 m (Štorch 1998). Some of the sills, however, apparently reached to a few meters below the water-sediment interface, as indicated by intraclasts of Silurian basalts embedded within contemporaneous shallow-water sediments (Štorch, pers. comm. 1997). The Lower Paleozoic sequence was later buried to the depth of the oil/gas window and subjected to burial temperatures in the range 90–180 °C (Suchý and Rozkošný 1996).

Samples for the present study were collected at the Kosov Quarry, Beroun County (Fig. 1). Exceptionally large, three-dimensional exposures at this locality enable the detailed study of a series of basalt sills that intruded pelitic sediments. The samples were collected both in the vicinity of several accessible sills and from apparently unaffected sediment (Fig. 2). The intrusions are generally bed-parallel and of variable thickness, ranging from about 40–50 cm up to 8–12 m. These igneous rocks, known as "diabases" in older literature, have been classified as doleritic basalts (Fiala 1970), or trachybasalts (hawaiites) in accordance with the classification of Le Maitre (1985; see also Štorch 1998 and the discussion therein). A 4 m thick sill exposed on the third level of the quarry was studied in detail (see Fig. 2). The mineralogy of this particular intrusive body has already been examined by Šrámek and Mráz (1984; the intrusion of "chloritized diabase" shown in their Photo 2). The adjacent sediments that were affected by the intrusions were black, graptolite shales of the Liteň Formation (Lower Silurian). There was also minor intrusion of the sills into the overlying Kopanina Formation, which consists of calcareous and tuffitic shales. Detailed mineralogi-

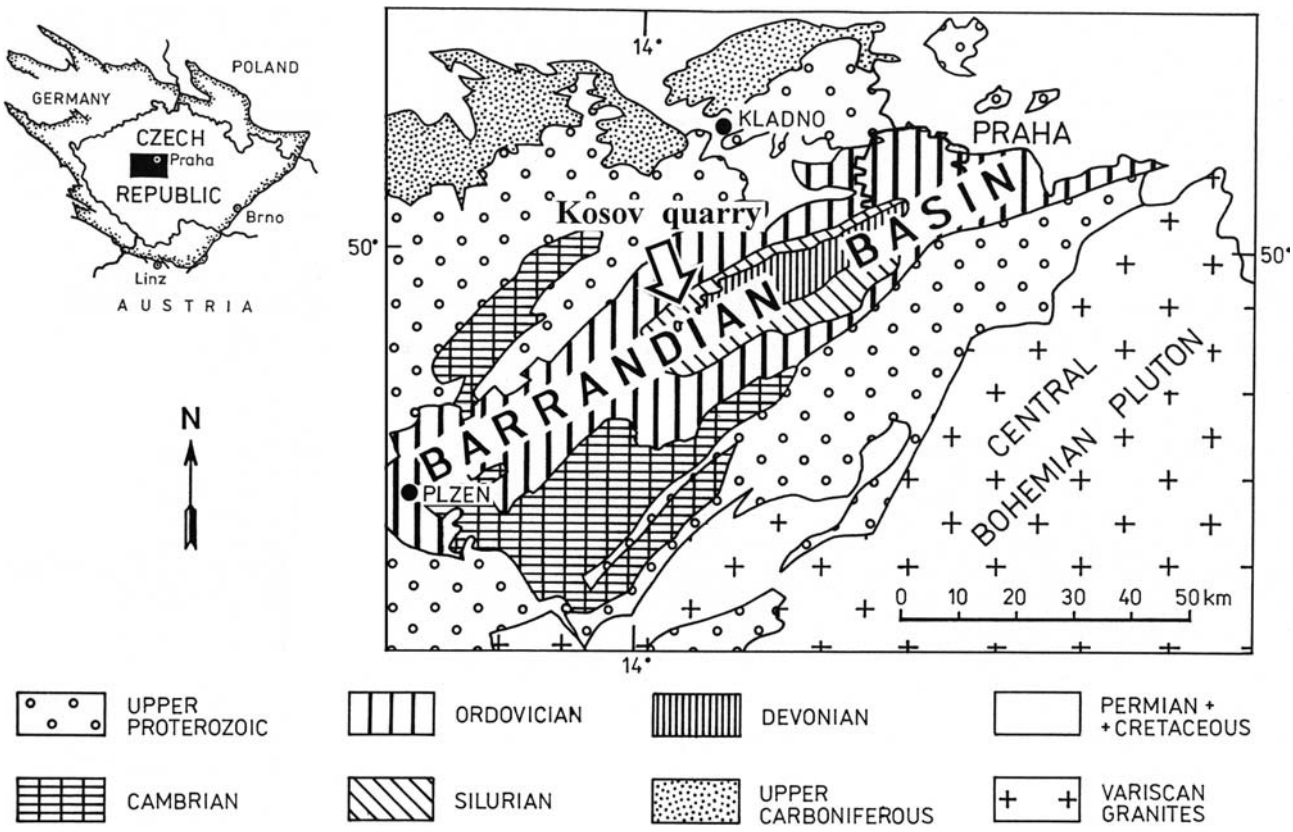

Figure 1. Simplified geological map of the Barrandian Basin and the location of the study area.

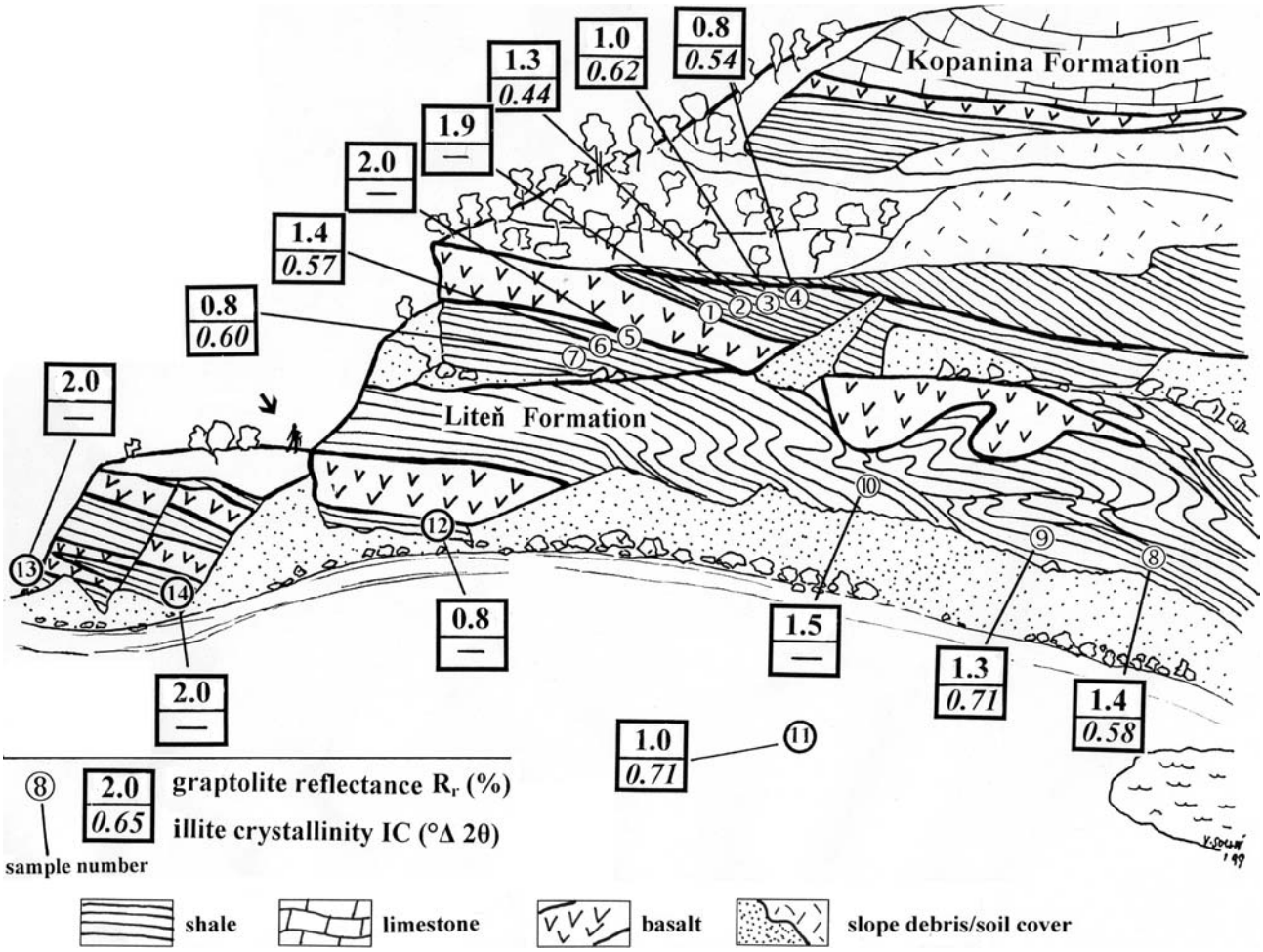

Figure 2. Schematic view of the northeastern face of the Kosov quarry, showing the location of the sills and the samples studied. The values of organic matter reflectance and illite crystallinity have also been plotted. A human figure (indicated by an arrow) is shown for scale.

cal and geochemical data on these shales can be found elsewhere (Štorch and Pašava 1989, Volk et al. 1999).

Experimental procedures

Reflectance data were collected on graptolite-rich shale samples cut and polished in sections perpendicular to bedding. The Opton-Zeiss UMSP 30 microscope equipped with a reflected white light source was used for photometric measurements. Random, maximum, and minimum reflectance values of graptolite fragments were determined using immersion objectives (magnification 40× and 100×) under oil (n = 1.518), in monochromatic and polarized light (λ = 546 nm). The reflectance values were measured on homogeneous spots of the graptolite cortex. Bireflectance was calculated as the difference between the measured maximum and minimum reflectance values.

Infrared spectra of graptolite fragments were collected using a Nicolet Magna 700 FT-IR spectrometer coupled with a Spectra Tech infrared microscope (MCD detector). The shale samples were cut perpendicular to bedding, and polished to provide a smooth surface for analysis. FT-IR spectra were collected from 20 × 10 μm areas. The background spectra were obtained from a gold-coated mirror. The measurements were made in reflectance mode, converted into the Kubelka–Munk scale and subjected to standard spectral processing (smoothing, curve fitting, and resolution).

Micro-Raman spectroscopy was performed on the polished samples used for organic matter reflectance measurements. A Raman LabRam HR apparatus (Jobin Yvon) linked to an Olympus microscope, fitted with a 100× objective placed on an X-Y motorized sample stage, was used. The 532 nm line of an Ar-ion laser was employed with a source power of 0.50 mW. Such low incident power is required to avoid the *in situ* maturation of the sample and the generation of spectral artifacts (Everall et al. 1991). The area of the measurements was approximately 1μm in diameter, with the depth of analysis within the sample being also about 1 μm (Lespade et al. 1984). The scattered light was analysed by a spectrograph with holographic grating of 600 g/mm, a slit width of 150 μm, and an opened confocal hole of 1000 μm. The positioning of the system was regularly checked using a silicon sample and by measuring the zero-order position of the grating. The acquisition time of particular spectral windows was optimized for individual sample measurements (about 3 seconds). Twenty accumu-

lations were co-added to obtain a spectrum. The Raman spectra of the samples were fitted using two Lorentzian lines around 1360 cm^{-1} (D band) and 1600 cm^{-1} (G band), and a broad Gaussian band at about 1540–1550 cm^{-1}: that are assigned to the graphitic phase (Tuinstra and Koening 1970, Bustin et al. 1995).

Gas chromatograph mass spectrometry (GC-MS) was applied to selected shale samples in order to reveal the chemical composition of organic fluids extracted from the sediment. Small, fresh rock chips were cleaned and crushed in an annealed agate mortar and extracted with purified *n*-hexane for 24 hours at room temperature. After multiple treatments the extracts (20 ml) were analysed on GC-MS. No separation of the extracts into saturated and aromatic parts was done. The instrumental conditions of the GC Hewlett Packard 5671 were as follows: capillary column DB5–30 m × 0.32 mm, helium as carrier gas, 20 cm/min, thermal gradient 50–310 °C.

To trace the thermal evolution of the clay minerals, illite crystallinity [IC; i.e. the full-width-at-half-maximum (FWHM) of the first 10 Å basal reflection of illite-muscovite] and chlorite crystallinity indices [i.e. the FWHM values of the second (7Å) basal reflection of chlorite indicated as ChC] were determined by XRD method. The measurements were performed on air-dried < 2 μm clay suspensions, pipetted onto glass slides (~2 mg/cm^2). Prior to slide preparation, carbonates were removed by treatment with cold CH_3COOH 5%. XRD measurements were performed using a Philips X'Pert X-ray diffractometer with computerized APD system, operated at 40 kV and 40 mA (Cu-K_α radiation, proportional counter, graphite monochromator), and with 0.5°/0.1°/0.5° mm slits. Samples were scanned from 7 to 11° 2θ (illite) and from 11 to 13° 2θ (chlorite) at a speed of 1°/min. The mean of several crystallinity measurements was calculated, and the average standard deviation was 0.017° Δ2θ. The calibration of IC and ChC values against Kübler's IC scale, where the anchizone ranges between 0.25 and 0.42° Δ2θ for air-dried samples, was made using a set of the Crystallinity Index Standards (CIS) of Warr and Rice (1993 and 1994). Applying the least square method, the calibration equation was as follows: IC (calibrated CIS data) = 0.894 · IC (present work) + 0.100 (R^2 = = 0.942).

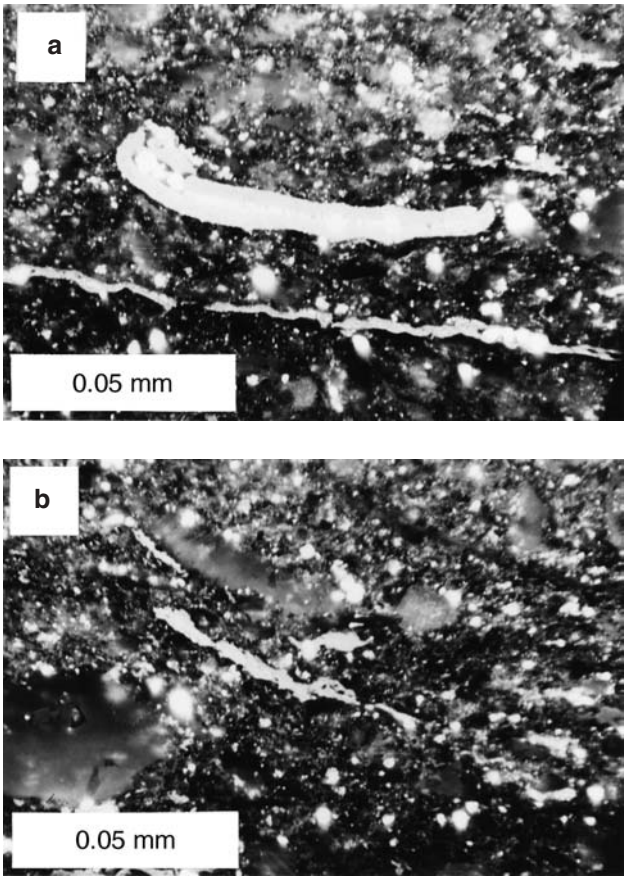

Figure 3. Photomicrographs showing typical optical features of graptolite particles in shales adjacent to a 4m thick basalt intrusion. See also Fig. 2 for the exact position of the samples shown. Reflected light, oil immersion.
a – sample No. 3; 1.7 m above the intrusion. R_r = 1.0%, R_{max} = 1.8%. Brightly-reflecting circular bodies inside the graptolite chamber and in the adjacent shale matrix are framboidal sulfides. b – sample No. 5; the lower contact. R_r = 2.0%, R_{max} = 3.6%. Note the optically inhomogenous, slightly undulatory-extinct internal fabrics of a graptolite particle, which is indicative of elevated thermal maturity.

The influence of the cooling magma on the intruded sediments was estimated by the following transient heat conduction equation in a model with an axi-symmetric geometry:

$$c\rho\partial T/\partial t = \partial/\partial z(k\partial T/\partial z) + k/r^* \partial T/\partial r + \partial/\partial r(k\partial T/\partial r) + A$$

where:
T is temperature, t time, c specific heat, ρ density, z depth, r distance (radius) from the axis of symmetry, k thermal conductivity, and A the heat production of the rocks. The solidification was assumed to occur between the temperature of liquidus T_l and solidus T_s, with the gradual release of the heat of crystallization L. The latter process was taken into account by increasing the specific heat of the magma (Carslaw and Jaeger 1959) by $L/(T_l - T_s)$ within the melting range (T_s, T_l). The emplacement of the molten layer was considered to be instantaneous and to have occurred at constant temperature, without any vertical displacement of the enclosing sediments. The equation was solved numerically by a computer code based on the finite difference method (Čermák et al. 1996). The performance of the code was checked by comparing the numerical solutions of similar problems involving melting, the analytical solutions of which are given in Carslaw and Jaeger (1959, p. 289). The sill was approximated by a vertical cylinder of 50 m diameter and 4 m in high. These dimensions seem to approximate the typical size of the intrusions present at the given locality. The magma feeding channel which is probably present below the sill was taken to have a diameter of 4 m (Fig. 9). The heat conduction equation was solved for a vertical cylinder with a radius of 500 m, so that the boundary conditions of horizontal symmetry applied at the cylinder surface did not influence solution in its axial part where the intrusion is located. The depth of the intrusion below the water-sediment interface was assumed to be in the range of 5–180 m, as follows from geological considerations. A surface temperature of 10 °C and a background terrestrial heat

flow of 60 mWm^{-2} at a depth of 500 m were the boundary conditions of the model. The thermal conductivity of the enclosing sediments at the time of the intrusive event was taken as 1 W . m^{-1}K^{-1}, a value typical for unconsolidated, water-saturated claystones (Galushkin 1997). The effect of possible hydrothermal fluid circulation above the intrusion (Peters et al. 1983, Krynauw et al. 1994) was simulated by elevating the conductivity of the sediments from 1 to 5 W . m^{-1}K^{-1} at the moment of sill formation (Fig. 9), thus simulating convective heat transport four times more intense than by conduction alone. A broad spectrum of initial magma temperatures was evaluated ranging from 900–1200 °C, typical of modern mafic magmas with a latent heat of crystallization of 3.8 . 10^5 J . kg^{-1} (Hanson and Barton 1989, Galushkin 1997), down to a minimum conceivable temperature of emplacement of 600–700 °C and zero latent heat. The initial temperature at the contacts was assumed to be an average of the magma temperature and the temperature of the adjacent rock.

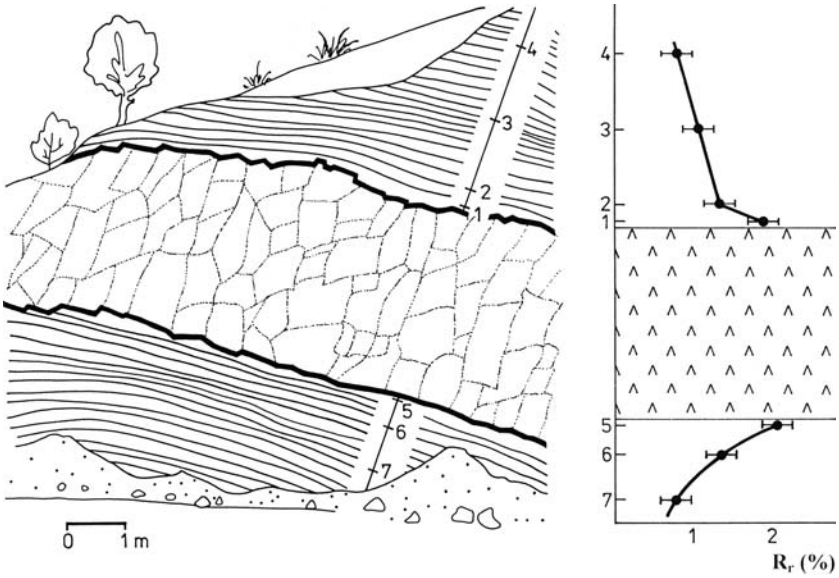

Figure 4. Field sketch showing the geometry of a 4 m thick diabase sill, the position of samples studied, and the coalification aureole around the sill as defined by random reflectance of graptolites.

Results and interpretations

Reflected light microscopy

Graptolites were the most abundant type of organic matter in the shale; it was therefore on these organic particles that all reflectance measurements reported in this paper were carried out (Fig. 3). Graptolite reflectance data can be correlated with vitrinite reflectance, thus enabling the degree of organic maturation to be accurately assessed (Goodarzi 1990, Cole 1994, Gentzis et al. 1996 among many others). The random reflectance of graptolites ranges from about 0.8 % to 2.0 % R$_r$, which corresponds to maximum reflectance values of about 1.8 % to 3.6 %, respectively. Graptolite reflectance rises from the regional background level, which can be as low as 0.8 to 1.0 % R$_r$. It is apparent that the reflectance values only rise to more substantial levels in the immediate vicinity of the sediment-intrusion contacts (Fig. 4 and Fig. 5a). Graptolite bireflectance also increases to 3.1 % close to the basalt contacts, probably as a consequence of the rapid rock heating during the intrusive event (Table 1). The symmetrical pattern of reflectance profiles above and below the sills indicates that the heating was comparable along both igneous contacts and/or only slightly higher above the upper contact of the sills.

The measured graptolite reflectance values were converted into vitrinite reflectance equivalents using the equations proposed by Bertrand (1990, Figs. 5 and 6), Hoffknecht (1991, Fig. 48), and Cole (1994). The respective vitrinite reflectance equivalent values at the contacts are in the range of 1.20 to 2.0 % R$_r$. In rapidly heated, liquid-dominated geothermal systems, these vitrinite reflectance values are characteristic of temperatures between 140 and 220 °C (Barker 1983). In contrast, graptolite reflectance values measured away from the igneous bodies that correspond to the burial-related "diagenetic background" (0.8–1.0 % R$_r$) are characteristic of temperatures around ~80–90 °C (Suchý and Rozkošný 1996).

Table 1. Summary of graptolite reflectance and clay mineral crystallinity values for the samples from Kosov quarry. See Fig. 2 and Fig. 4 for the location of individual samples

Sample number	R$_r$ (%)	R$_{max}$ (%)	R$_{min}$ (%)	Bireflectance (%)(R$_{max}$ – R$_{min}$)	IC (°Δ2θ)	ChC (°Δ2θ)
1	1.9	3.0	0.8	2.2	–	–
2	1.3	1.7	1.0	0.7	0.44	0.34
3	1.0	1.8	0.6	1.2	0.62	0.38
4	0.8	1.8	0.4	1.4	0.54	0.37
5	2.0	3.6	0.5	3.1	–	–
6	1.4	2.2	0.9	1.3	0.57	0.37
7	0.8	2.0	0.5	1.5	0.60	0.36
8	1.4	2.2	0.7	1.5	0.58	0.30
9	1.3	1.9	0.7	1.2	0.71	0.36
10	1.5	2.4	0.7	1.7	–	–
11	1.0	1.8	0.6	1.2	0.71	–
12	0.8	2.0	0.6	1.4	–	–
13	2.0	3.2	1.2	2.0	–	–
14	2.0	3.3	0.8	2.5	–	–

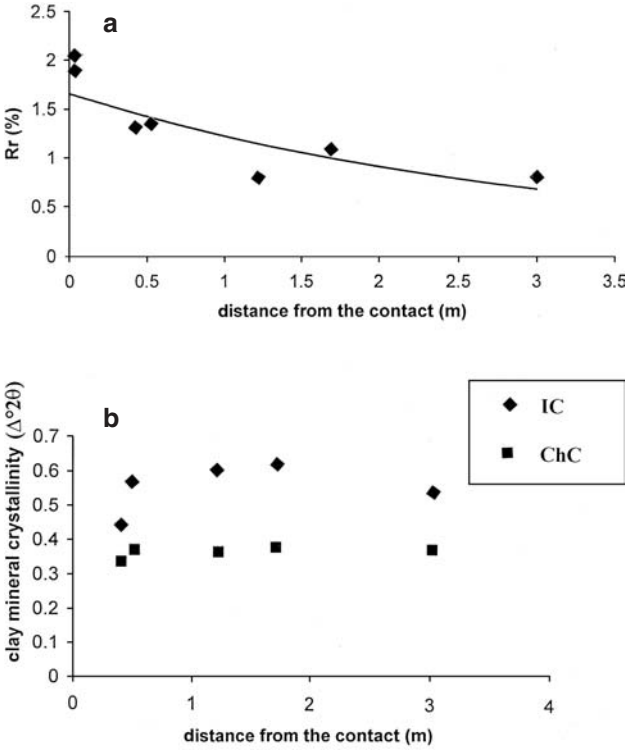

Figure 5. Graptolite reflectance (a) and illite/chlorite crystallinity values (b) as a function of distance from the intrusive contact of a 4 m thick basalt sill. See text for details.

Micro Fourier-Transform infrared spectroscopy (FT-IR)

FT-IR was applied to examine the chemical composition and thermal exposure of a series of graptolite samples, varying in reflectance from 0.8% to 2.0% R_r (Fig. 6). Aside from the spectra of graptolite organic constituents, contributions from the minerals of the enclosing rock, such as calcite, quartz, and illite, were also recorded in most samples. The typical spectra of graptolite fragments are similar to those of higher rank coals or kerogens which exhibit a broad asymmetric peak around 3600 cm^{-1}, ascribed to OH hydroxyl groups (see also Rouxhet et al. 1980, Tissot and Welte 1984, and Ibarra et al. 1996 for the typical FT-IR spectra of various coaly materials). We interpret another distinct peak around 1600 cm^{-1} in terms of skeletal aromatic C=C bonds. A band at 1235 cm^{-1} is believed to be associated with C-O bending vibrations, and O-H group deformation vibrations. The spectral area between 2800 and 3000 cm^{-1}, particularly the CH_3 (2960 cm^{-1})/CH_2 (2930 cm^{-1}) intensity ratio, which involves C-H stretching and deformational vibrational bands, has petroleum-related significance (Rouxhet et al. 1980, Bustin et al. 1989, Lin and Ritz 1993). By examining seven representative graptolite samples collected at various distances from the intrusion, we found that the intensity ratio I_{2960}/I_{2930} closely correlates with the respective R_r values of graptolite reflectance (Fig. 7). This shows that with increasing thermal exposure closer to the igneous body, the aliphatic C-H bonds tend to vanish and the graptolite periderm is gradually converted into a condensed aromatic residuum similar to highly matured coals and/or kerogens. Moreover, a close link between the I_{2960}/I_{2930} intensity ratio and graptolite reflectance, as shown in Fig. 7, implies that with increasing thermal stress, structural and chemical changes of graptolite material correlate closely with its optical change.

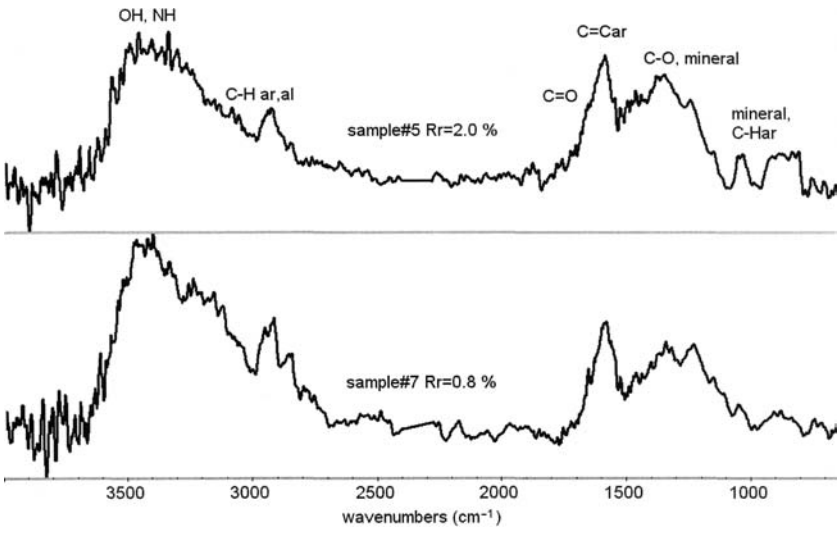

Figure 6. Representative FT-IR spectra of two graptolite samples of contrasting thermal maturity affected by the intrusive heat. See text for details.

Micro-Raman spectrometry

This method was applied to three graptolites of contrasting maturity (from R_r 0.80% to1.90%) toward providing further information on heat-induced changes in the structure of the graptolite material. The results are summarized in Table 2, and the representative first-order spectra are shown in Fig. 8 together with the reference spectrum of structurally well-ordered natural graphite. All three samples exhibit prominent Raman peaks centered at relative wave numbers of approximately 1356 and 1595 cm^{-1} (Fig. 8). Pure graphite, on the other hand, has a single Raman peak centered at 1575 cm^{-1}, though increasing disorder within planar and stacking lamellae produces a gradual shift and broadening of this peak to around 1578 cm^{-1} (the so-called G band) in addition to the appearance of a smaller disorder-induced peak near 1352 cm^{-1} (the so-called D band; Tuinstra and Koenig 1970, Wopenka and Pasteris 1993). The latter typically arises when the crystallite size of the graphite decreases below some minimum value; its development is therefore a reliable indicator of the degree of disorder in the material (Lespade et al. 1982, Kříbek et al. 1994). The A_D/A_G ratio between the 1600 and 1350 cm^{-1} peaks, expressed in terms of their integrated areas, was used to characterize the difference between individual types of carbonaceous matter

(Table 2). The spectral characteristics of the two "end member" graptolite samples collected at the upper igneous contact (sample No. 1) and 3 meters above the intrusive body, respectively (sample No. 4) are generally consistent with these predicted variations, showing a significant reduction in the line-width around ~1600 cm^{-1} (G bend) of the higher rank sample (1.9 % R_r). This change points to increased order within the graptolite structure with increasing thermal maturity toward the igneous sill. A similar relationship has already been observed for other carbonaceous materials subjected to thermal metamorphism, including coals (Beny-Bassez and Rouzaud 1985) and chitinozoans (Roberts et al. 1995). Although the present results of the micro-Raman spectroscopy of graptolites are too few to be directly compared with reflectance data, they clearly indicate that the A_D/A_G (1350/1600 cm^{-1}) peak area can potentially complement existing techniques for indicating the maturity of sedimentary rocks by correlating optical methods of assessing thermal maturity with the physical and chemical changes that occur at the microscopic level.

Gas chromatography-mass spectroscopy (GC-MS)

GC-MS was employed to investigate the extracts of three representative shale samples from below the intrusive contact, and those coming from unaffected sediments. Though the number of samples was limited, the analyses provided interesting clues to the thermal history of the intrusion and the enclosing strata. We found elevated contents of *n*-hexane – extractable hydrocarbons in the contact zone of the sill, which fall to only 0.006 wt.% at the sill contact, a reduction from the background level of about 80% (Table 3). Similar appreciable loss of organic matter adjacent to the intrusion has already been observed in contact aureoles elsewhere and explained by the rapid gasification of organic matter in the host shale at severe thermal conditions (Perregaard and Schiener 1979, Saxby and Stephenson 1987). It is probable that subsequent to the intrusion event, the samples nearest to the igneous body were at high temperatures (600–700 °C)

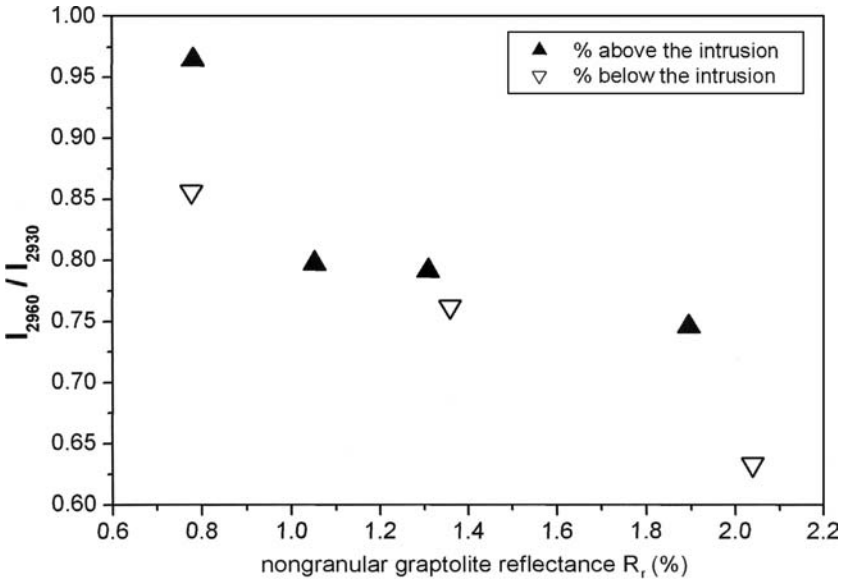

Figure 7. CH_3 (2960 cm^{-1})/CH_2 (2930 cm^{-1}) integrated intensity ratio versus optical reflectance for a series of graptolite fragments collected at various distances from a 4 m thick basalt intrusion. See text for discussion.

Table 2. Band area ratios (A_D/A_G) between the 1600 and 1350 cm^{-1} peaks in Raman spectra and respective optical reflectance values for two representative graptolite samples around the intrusion. See also Fig. 4 for the position of the samples in the section studied

Sample number	Rr (%)	Peak position (cm^{-1})	Bandwidth (cm^{-1})	Band area ratio A_D/A_G
1 (upper contact)	1.9	1348 (D band)	267	4.26
		1597 (G band)	61	
6 (0.5 m below the sill)	1.4	1348 (D band)	266	4.28
		1597 (G band)	62	
4 (3 m above the sill)	0.8	1347 (D band)	238	5.04
		1600 (G band)	68	

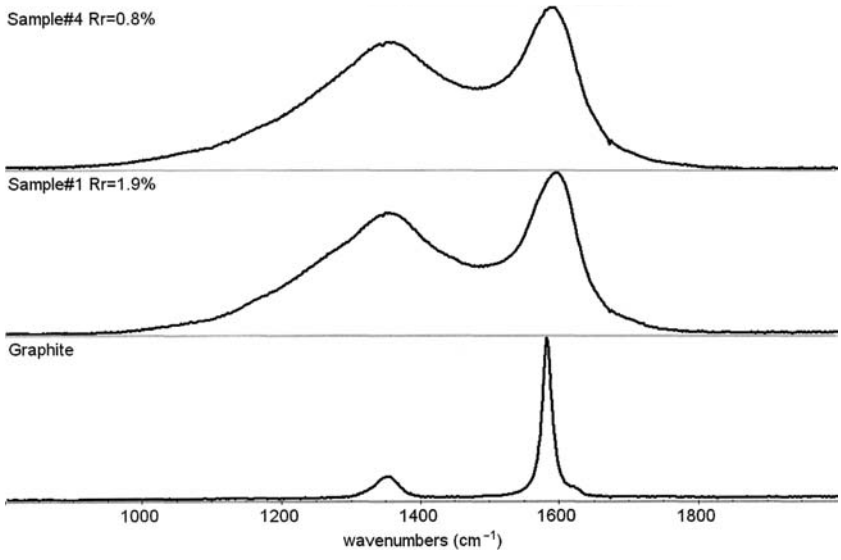

Figure 8. First-order Raman spectra obtained from graptolites of 0.8 and 1.9 % R_r rank, showing characteristic bands at ~ 350 and ~1600 cm^{-1} for carbonaceous material. Note the significant reduction in the line-width of the 1600 cm^{-1} (G band) of the higher rank (1.9 %) analysis. For comparison, the spectrum of well-ordered graphite from the Vyšný Lazec graphite deposit (Moldanubian Zone, Czech Republic) is also shown (adopted from Kříbek et al. 1994).

Table 3. Pristane-to-phytane (Pr/Ph), Pr/n-C_{17}, Ph/n-C_{18} and CPI ratios for four representative black shale samples adjacent to the sill. The ratios of phenanthrene and alkylphenanthrene biomarkers of samples 5, 6, and 7 are also given.

Sample number	R_r (%)	Pr/Ph	Pr/n-C_{17}	Ph/n-C_{18}	CPI	MPI-1	MPI-3	MPR	MP/P	DMPI
5 (lower contact)	2.0	0.40	0.032	0.093	1.180	–	–	–	–	–
6 (0.5 m below the sill)	1.4	0.13	0.021	0.153	1.087	0.93	1.03	1.63	0.36	0.35
7 (1.2 m below the) sill	0.8	0.15	0.028	0.189	1.218	0.91	1.00	1.52	0.33	0.33
4 (unaffected sample)	0.8	0.78	0.140	0.270	1.043	–	–	–	–	–

and contained steam from the sediment pore waters and/or the magma itself. The organic carbon in the sediments at the contact may have reacted with steam, the clay minerals acting as potential catalysts, resulting in the formation of carbon monoxide and hydrogen (i.e. so-called synthetic gas that is commonly produced on a commercial basis; Bishop and Abbot 1995). In contrast to the contact sample, a particularly large *n*-hexane extract (0.105 wt.%) was obtained from a sample collected 1.2 m below the intrusion, which yielded a concentration about three times higher than in unaltered Liteň shale samples (Table 3). This observation suggests that pyrolytic products from the black shale below the intrusion diffused or were driven away from the contact and trapped in what can be called a "micro-reservoir" (e.g. Saxby and Stephenson 1987), probably because the surrounding rock was cool enough to allow the vapours to condensate.

The pristane-to-phytane (Pr/Ph) ratio of the unaffected Liteň shale is about 0.78, which is typical for oil-window conditions (Suchý et al. 2002). Comparably low Pr/Ph ratios of less than 1 typically occur in some organic-rich anoxic sequences (Powell and McKirdy 1973), or in some oils generated from Paleozoic carbonate source rocks (Illich and Grizzle 1983). The samples affected by igneous heat yielded Pr/Ph values that were appreciably lower than those of unaltered sediments. This was unexpected, because Pr/Ph ratios generally increase with increasing degree of maturity (e.g. Powell and McKirdy 1973). Thus the variation in Pr/Ph ratios may be related to the rapid heating experienced by the shale horizon (Boudou 1984, George 1992). The influence of the maturation process increasing toward the igneous body is followed by systematically decreasing Pr/*n*-C_{17} and Ph/*n*-C_{18} ratios, which are frequently used as alternative temperature indicators of maturity (Tissot and Welte 1984). There is particularly marked gradient in Ph/*n*-C_{18} ratios from 0.27 in the sample of lowest maturity (1.0% R_r) to 0.093 in the most highly mature sample (2.0% R_r) at the igneous contact. The gradual decrease of this value toward the intrusion indicates the heat-controlled conversion of a thermodynamically unstable branched phytane (C_{20}), which grades into a more stable *n*-octadecane.

The isolated *n*-alkane fractions are within the nC_{13}–nC_{30} range, with a maximum between nC_{17}–nC_{19} that shows no obvious trend with respect to the contact aureole. A slight odd/even predominance can be detected in all the samples within the zone of influence as far as 1.2 m away from the contact (CPI = 1.218). Beyond that limit, the *n*-alkane extracts exhibit lower CPI values that correspond to unaltered Liteň shale at a vitrinite reflectance level of about 1.2–1.4% R_r (Hunt 1996).

The presence of terpane and sterane biomarkers is restricted to the samples furthest from the igneous contact. The terpanes were identified only at a distance of 0.5 m away from the contact, whereas both terpane and sterane biomarkers were found only 1.2 m away from the sill (Table 3), indicating maturity of the host rock equivalent to a vitrinite reflectance of about 1.25% R_r (Mackenzie 1984). Aromatic biomarkers dominated by thermodynamically more stable β-derivates, including phenanthrene, metylphenanthrene, and dimethylphenanthrene were also identified only in samples distant from the contact, suggesting that closer to the sill these thermally-sensitive hydrocarbons were probably pyrolyzed or otherwise thermally degraded.

Clay mineral diagenesis

The Liteň black shales that host most of the intrusions are mineralogically uniform. Illite is present in all samples studied, with the majority containing chlorite. Variable amounts of quartz, Na-Ca feldspar, calcite, and rare dolomite were recognized as accessory phases in most samples. The proportions of individual mineral constituents show no apparent correlation with distance from the igneous contacts. Nevertheless, the samples collected from the igneous contacts appear to contain higher amounts of plagioclase and appreciably lower amounts of chlorite relative to those from outside the contacts. In both contact samples a small amount of smectite has been detected coexisting with illite.

In the samples studied for this project, *illite crystallinity (IC)* data depict a medium to high-grade diagenetic stage with Kübler index (IC) values ranging from 0.70° to 0.44° Δ2θ (Table 1). The lowest crystallinity values (i.e. the highest IC values; ~ 0.70–0.60° Δ2θ) were measured in samples distant from the basalt intrusions. Since similar IC values are typical for Silurian sediments elsewhere in the basin that were not affected by contact metamorphism (Suchý and Rozkošný 1996), these values probably represent the "diagenetic background" and can be interpreted in terms of burial heating alone. The samples collected closer to the basalt intrusions had higher crystallinity values (up

to 0.44° Δ2θ), and must have been affected by intrusive heating. Elevated illite crystallinity, however, has been detected only in a relatively narrow zone immediately adjacent to the igneous contacts. In the case of a 4 m thick basalt sill, for instance, the zone in which elevated IC values were identified was only about 0.5 m thick (Fig. 5b).

A limited number of *chlorite crystallinity (ChC)* values obtained over the Kosov quarry show variations similar to, though less decisive than, those of the illite crystallinity index (Table 1). The 7Å ChC values generally range from 0.37° to 0.30° Δ2θ, which suggests medium to high-grade diagenetic conditions (Árkai 1991). In some cases, the samples located close to the intrusive bodies tend to possess improved chlorite crystallinity compared to those far outside the intrusions. In general, however, the differences in ChC values between the individual samples apparently affected by intrusive heat are relatively small (Fig. 5b). This observation seems to confirm the conclusion of some workers that the ChC method is a less sensitive tool than the IC method, as 7Å ChC increases more sluggishly than IC during advanced diagenesis (Árkai et al. 1995, Yang and Hesse 1991).

Various relationships between temperatures and IC and/or ChC values have been proposed (Frey et al. 1980, Árkai 1991, Underwood et al. 1992, Mullis et al.1995, Kosakowski et al. 1999). According to these studies, the highest IC values that are characteristic of the Kosov contact-metamorphic samples (about 0.44° Δ2θ) may correspond to temperatures between 170–230 °C, though more recent empirical observations from active geothermal fields suggest substantially higher temperatures in the range of 275–300 °C (Junfeng Ji and Browne 2000). The highest chlorite crystallinity values (0.34–0.30° Δ2θ, encountered in samples 2 and 8 respectively) can be interpreted in terms of temperatures ranging from 200 to 240 °C, according to the correlation chart of Árkai (1991, Fig. 5).

Thermal modeling of the intrusion

In our modeling we have tested a number of initial magma temperatures ranging from 900–1200 °C to 600–700 °C. We also evaluated several geometrical distributions of the sills, though only one representative example is reported here: a calculation performed with a simple bed-parallel sill, 4 m thick, and entirely enclosed by organic-rich shale (Fig. 9).

Figure 10 illustrates the modeled thermal history of the complete igneous/sedimentary column at different times after the igneous event. In a scenario in which the initial temperature of the intrusion was 600 °C, the contacts were heated to 310 °C, and the heat carried to the surface by fluids was five times higher than the respective conductive heat flux. Each curve corresponds to temperature as a function of the depth, at an indicated time (in days and years) after the intrusive event. Maximum sediment temperatures around the intruded depth interval (180–184 m) range from 310 °C at the upper contact to 70 °C 10 m above the sill, and from 380 °C at the lower contact to 50 °C 10 m below the sill. These temperatures were attained almost immediately at the contacts, but required 2–3 years to migrate tens of meters away from the sill. The 1- and 5-year curves show that peak temperatures at the sill site decrease rapidly, and that heat is transferred to the sediments in the vicinity of the sill, smoothing out the spike to about 140 °C and 70 °C, respectively. Calculations also show that the temperature perturbation decays to a few degrees C above the background temperatures of 20 °C within 500 years. Similar but slightly higher temperatures were obtained assuming that the initial temperature of the intrusion was 700 °C. In that case peak sediment temperatures ranged from 360 °C at the upper contact to 77 °C 10 m above the sill, and from 440 °C at the lower contact to 59°C 10 m below the sill (Table 4).

After the igneous event, the sequence was subjected to burial at depth. As shown by independent geological indicators, the maximum burial temperatures in a given section may have reached 80–90 °C (Suchý and Rozkošný 1996, Dobeš et al. 1997). These later burial temperatures may have completely annealed the thermal effects of the intrusion at distances greater than 4–5 m below to 7–8 m above the igneous contacts, if the initial temperature of the intrusion was 600 °C. Alternatively, given an initial intrusion temperature of 700 °C, the complete annealing of the igne-

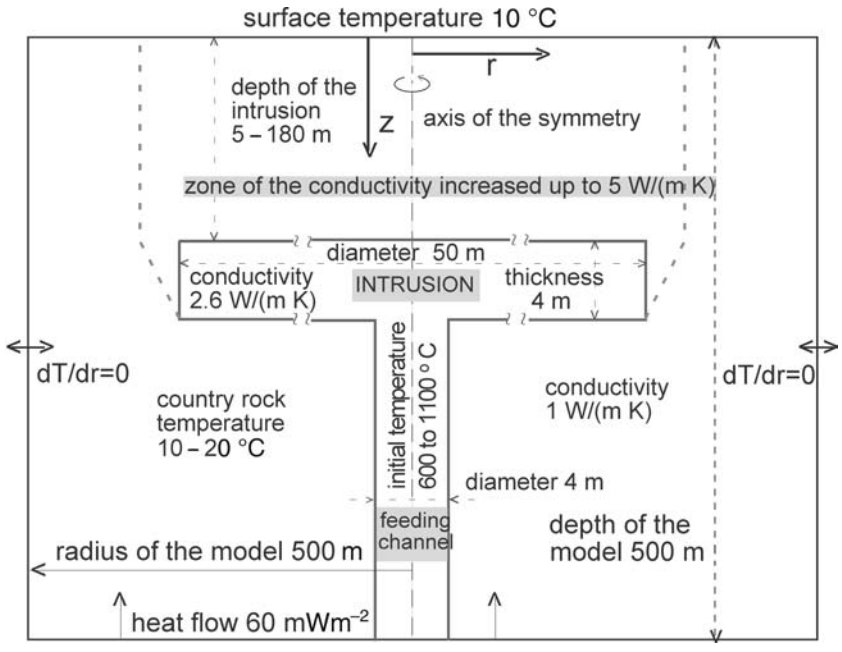

Figure 9. Vertical crosssection of the model of the intrusion, and the basic model parameters used for calculations. The intrusion was approximated by a vertical cylinder (50 m in diameter and 4 m thick) with a narrow magma chimney below its central part. Cooling by fluids was simulated by increased effective thermal conductivity above the ambient value of 1W . m^{-1} . K^{-1} to 5 W . m^{-1} . K^{-1}. See text for details.

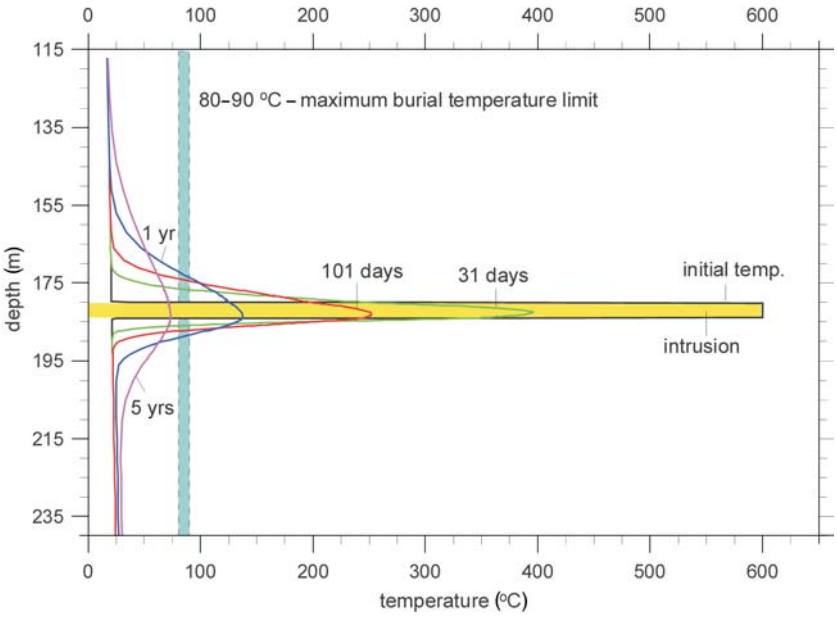

Figure 10. Calculated thermal profiles across the Kosov intrusion. The initial temperature of the intrusion was 600 °C. Each curve is designated with respective time after intrusion. Note the slight asymmetry of the thermal profile due to the elevated heat advection by fluids above the intrusion.

ous event by later burial heating would have occurred at the depths of 5–6 m below and 8–9 m above the intrusive body.

Figure 11 shows the time-temperature curves of the sediments enclosing the sill at various times after the emplacement of the intrusion. Each curve of this diagram displays the time-temperature path of an individual rock sample that has been examined for its organic and mineral diagenesis. Hydrothermal circulation that commonly occurs above sills (e.g. Krynauw et al. 1994) was approximated by applying elevated thermal conductivity to the section above the intrusion. The curves indicate that higher heat flux caused by hydrothermal circulation 3 m above the contact elevated the peak rock temperatures above the sill shortly after emplacement (sample 3.0a in Fig. 11). Over a longer time scale, however, hydrothermal circulation brought about the faster cooling of the entire host rock section. Hydrothermal cooling is especially apparent at the upper contact (see sample 0a in Fig. 11), where the temperature dropped from about 310 °C to 260 °C within 15 days. The curves for the rock 1.2 m below the igneous contact indicate that in this particular setting the hydrothermal regime may have caused lower peak rock temperatures (191 °C versus 207 °C) and the faster cooling.

According to our model, the duration of the heating event was relatively short. Intense heating lasted only some weeks to months after the emplacement of the sill. Given the hydrothermal cooling effects, the temperature perturbation of the section may have completely ceased within about three years.

Discussion

Natural geothermometers based on the "instantaneous" coalification of vitrinite and/or graptolite periderm (Bostick 1973, Bostick and Clayton 1986, Bustin et al. 1989) suggest maximum temperatures for the intrusive contacts within the range of 320–420 °C. Illite and chlorite crystallinity values indicate even lower maximum temperatures in the range of 170–300 °C, according to various empirical correlations (Árkai 1991, Mullis et al. 1995, Jungfeng Ji and Browne 2000 among many others). The discrepancy between the organic matter maturation and clay mineral crystallinity-based temperature estimates can probably be ascribed to the sluggish rate of the clay mineral reactions

Table 4. Calculated peak temperatures of individual samples from around the sill (shown in Fig. 4) and their respective temperature lifetimes. The initial temperature of the sill was taken as 600 or 700 °C. Two different values of the effective thermal conductivity (5 and 1 W . m^{-1} . K^{-1}) were used to simulate the thermal effects of hydrothermal circulation around the intrusion.

Sample number	R_r	600 °C, 1 W . m^{-1} . K^{-1}		600 °C, 5 W . m^{-1} .K^{-1}		700 °C, 1 W . m^{-1} . K^{-1}		700 °C, 5 W . m^{-1} . K^{-1}	
	(%)	T (°C)	time (days)	T (°C)	time (days)	T (°C)	time (days)	T (°C)	time (days)
4 (3 m above the sill)	0.8	133	311	139	109	152	311	159	109
3 (1.7 m above the sill)	1.0	178	157	171	63	205	157	197	63
2 (0.4 m above the sill)	1.3	288	38	229	23	334	38	265	23
1 (upper contact)	1.9	378	5	310	0	440	5	360	0
5 (lower contact)	2.0	378	5	378	5	440	5	440	5
6 (0.5 m below the sill)	1.4	273	45	265	35	317	45	307	35
7 (1.2 m below the sill)	0.8	207	105	191	77	239	105	220	77

(Hillier and Clayton 1989, Barker 1991, Olsson 1999). Nevertheless, all these empirical data generally suggest that the maximum temperatures of the sediments around the sill must have been remarkably low, relative to the initial temperature of mafic magmas that is typically as high as 900–1200 °C (Hanson and Barton 1989).

In our earlier computer simulations published elsewhere, we have shown that initial magma temperatures between 900–1200 °C would theoretically result in maximum contact temperatures up to 800 °C and extensive contact aureoles up to 10–12 times the thickness of the intrusion (see Šafanda et al., 2003 and the references therein). These computer simulations, however, clearly contradict to the empirical data of natural geothermometers that evince low temperatures and thin metamorphic aureoles. The new back-stepping computer simulations that we present in this study suggest that the initial temperature of the emplacement must have been as low as 600–700 °C to provide a reasonable match between the model and empirical data. In that case, the simulation results in peak temperatures of the sediments at the igneous contacts of only about 440 °C, and with contact aureoles of one to two times the thickness of the intrusion.

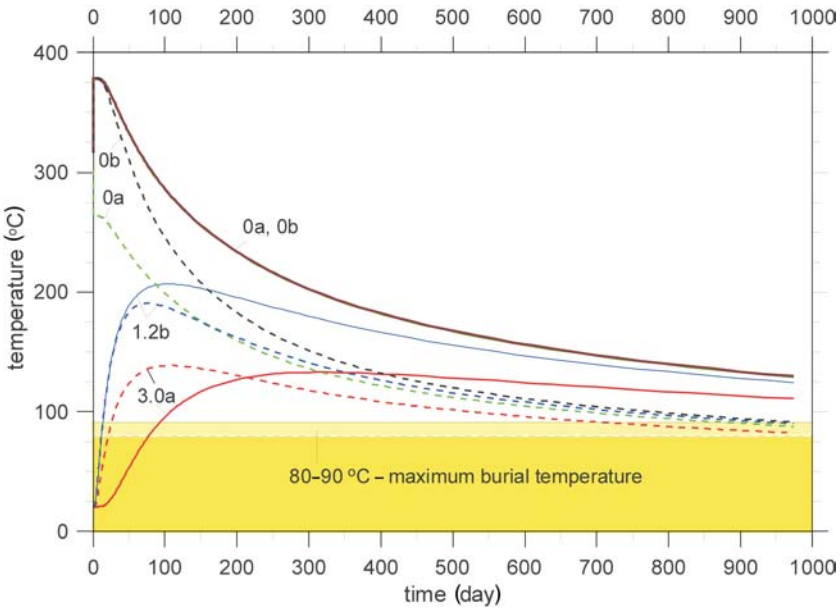

Figure 11. Calculated time-temperature curves at the upper (0a) and lower (0b) contacts, and 3 m above (3.0a) and 1.2 m below (1.2b) the sill, shown in full lines. The curves shown in dashed lines reflect the cooling effect of hydrothermal fluids. See text for details.

Our results from empirical data and computer simulations therefore imply that some mechanism must have existed that quickly removed heat from the intrusions without heating the enclosing sediments. Such effective cooling of the intrusions may have occurred due to surface waters. It is well known that some shallow submarine basalt intrusions interacting with seawater typically exhibit alteration at temperatures between 90 and 250 °C only, and generate contact aureoles merely a few centimeters thick (Rangin et al. 1983, Desprairies and Jehanno 1983, Coulon et al. 1985). A similar geological situation may have existed in the Barrandian basin. Field observations indicate that the Kosov sills were emplaced at a relatively shallow depth below the seafloor, into soft, unconsolidated, water-saturated clays. Independent petrophysical calculations have shown that the porosity of Kosov shales was still between 68–78% soon after deposition (Šrámek 1978). Nevertheless, some alternative explanations for the lowered temperatures near the igneous contacts are also viable. Galushkin (1997), for example, has suggested that if warm magma intrudes surrounding sediments within a shell of cooled magma, the temperatures involved may be considerably decreased. Another mechanism for reducing the contact metamorphic temperatures could perhaps have been the heat consumption due to dehydration reactions in the enclosing shale, as proposed by Hanson and Barton (1989), and Coombs (1993).

Conclusions

A series of thin sills of doleritic basalts that penetrated black Silurian shales at the Kosov quarry had only a limited influence on the maturity and diagenesis of the intruded sediments. Detailed research of a four-meter thick sill and the adjacent shales showed that moderately elevated values of graptolite reflectance developed close to the igneous contacts (1.9–2.0 % R_r corresponding to ~3.0–3.6 % R_{max}). The increase of the optical rank of graptolite tissue was accompanied by a depletion of aliphatic-containing groups and conversion into a condensed, relatively well-ordered carbonaceous residuum. In general, these transformations indicate short-lived contact metamorphic temperatures in the range of 140 °C to 420 °C that affected sediments adjacent to the sill. Following the magma emplacement, some of the extractable organic matter was instantly gasified by hot steam released from the magma and/or sediment pore waters, but some hydrocarbons apparently migrated away from the igneous body and condensed in a discrete "micro-reservoir" at a distance of about 1 m below the sill.

In contrast to the sensitive response of the organic materials, the intruded shale exhibits only limited increases in illite and chlorite crystallinity (IC = 0.44° $\Delta 2\theta$; ChC = = 0.34° $\Delta 2\theta$) within the contact aureole. This can be explained in terms of a "lag" of mineral diagenesis behind the organic metamorphism.

The thermal evolution of the sill in time and space was modeled using an unsteady state heat conduction equation. The modeling gives contact temperatures that are reasonably close to those derived from independent paleothermal indices, given that the magma was highly water-saturated and its temperature did not exceed 600–700 °C. Surface waters quickly cooled the sill that probably caused the lim-

ited extent of the thermal alteration and the low maximum temperature experienced by the enclosing sediments.

Acknowledgements. This study was supported by research grants A3012703/1997 (to J. Š.), K2067107 (to I. S.), and MSM 223200003 (to M. S.), kindly provided by the Grant Agency of the Academy of Sciences and the Ministry of Education, Youth and Sport of the Czech Republic respectively. All financial contributions are gratefully acknowledged. Comprehensive reviews of the manuscript by Dr. S. Vrána (Czech Geological Survey) and an anonymous referee were helpful and made a significant contribution to the final form of the paper. Dr. Simon C. George (CSIRO Petroleum, Sydney, Australia) and Dr. Neely H. Bostick (U.S. Geological Survey, Denver, Colorado) are thanked for their constructive comments on an earlier version of this paper and for grammatical improvements. Dr. Šárka Eckhardtová and Dr. Marie Lachmanová (both formerly of Geological Institute AS CR) kindly provided technical assistance during organic matter reflectance measurements and time-consuming separations of clay minerals, respectively. The company Cement Bohemia, a. s., allowed us to undertake field sampling at the Kosov Quarry.

References

Árkai P. (1991): Chlorite crystallinity: an empirical approach and correlation with illite crystallinity, coal rank and mineral facies as exemplified by Palaeozoic and Mesozoic rocks of northeast Hungary. J. Metamorphic Geol. 9, 723–734.

Árkai P., Sassi F. P., Sassi R. (1995): Simultaneous measurements of chlorite and illite crystallinity: a more reliable tool for monitoring low- to very low grade metamorphism in metapelites. A case study from the Southern Alps (NE Italy). European J. Mineral. 7, 1115–1128.

Barker C. E. (1983): Influence of time on metamorphism of sedimentary organic matter in liquid-dominated systems, western North America. Geology 11, 384–388.

Barker C. E. (1991): Implication for organic maturation studies of evidence for a geologically rapid increase and stabilization of vitrinite reflectance at peak temperature: Cerro Prieto Geothermal System, Mexico. Amer. Assoc. Petrol. Geol. Bull. 75, 1852–1863.

Beny-Bassez C., Rouzaud J. N. (1985): Characterization of carbonaceous matter by correlated electron and optical microscopy and Raman microspectrometry. Scanning Electron Microscopy 1, 119–132.

Bertrand R. (1990): Correlations among the reflectances of vitrinite, chitinozoans, graptolites and scolecodonts. Org. Geochem. 15, 565–574.

Bishop A. N., Abbot G. D. (1995): Vitrinite reflectance and molecular geochemistry of Jurassic sediments: the influence of heating by Tertiary dykes (northwest Scotland). Org. Geochem. 22, 165–177.

Bostick N. H. (1973): Time as a factor in thermal metamorphism of phytoclasts (coaly particles). In: Septième Congrès Internat. de Stratigraphie et de Géologie du Carbonifère, Krefeld, 1971; Compte Rendu 2, 183–192.

Bostick N. H., Clayton J. L. (1986): Organic petrology applied to study of thermal history and organic geochemistry of igneous contact zones and ore deposits in sedimentary rocks. In: Dean W. E. (ed) Organics and Ore Deposits, Proceedings of the Denver Exploration Geologists Society Symposium, April 1985, 33–55.

Boudou J. P. (1984): Chloroform extracts of a series of coals from Mahakam Delta. Org. Geochem. 6, 431–437.

Bustin R. M., Link C., Goodarzi F. (1989): Optical properties and chemistry of graptolite periderm following laboratory simulated maturation. Org. Geochem. 14, 355–364.

Bustin R. M., Ross J.V., Rouzaud J. N. (1995): Mechanisms of graphite formation from kerogen: experimental evidence. Int. J. Coal Geology 28, 1–36.

Carslaw H. S., Jaeger J. C. (1959): Conduction of Heat in Solids, 2nd ed. Oxford Univ. Press, London.

Čermák V., Šafanda J., Kresl M., Kučerová L. (1996): Heat flow studies in Central Europe with special emphasis on data from former Czechoslovakia. Tectonics and Metallogeny 5, 109–123.

Chlupáč I., Havlíček V., Kříž J., Kukal Z., Štorch P. (1998): Palaeozoic of the Barrandian (Cambrian to Devonian). Czech Geological Survey, Prague.

Cole G. A. (1994): Graptolite-chitinozoan reflectance and its relationship to other maturity indicators in the Silurian Quasaiba Shale, Saudi Arabia. Energy and Fuels 8, 1443–1459.

Coombs D. C. (1993): Dehydration veins in diagenetic and very-low-grade metamorphic rocks: Features of the crustal seismogenic zone and their significance to mineral facies. J. Metamorphic Geol. 11, 389–399.

Coulon H., Debrabant P., Lefèvre C. (1985): Données pétrographiques, minéralogiques et géochimiques sur la transition basaltes – sédiments dans l'Atlantique Nord. Ann. Soc. géol. Nord 104, 219–233.

Desprairies A., Jehanno C., (1983): Paragenèses minérales liées à des interaction basalte – sédiment – eau de mer (sites 465 et 456 des legs 65 et 60 du D.S.D.P.). Sci géol. Bull. Strasbourg 36, 93–110.

Dobeš P., Suchý V., Sedláčková V., Stanišová N. (1997): Hydrocarbon fluid inclusions from fissure quartz: a case study from the Barrandian basin (Lower Paleozoic), Czech Republic. In: Boiron M. C., Pironon J. (eds) XIV ECROFI; Proceedings of the XIVth European current research on fluid inclusions, volume de resumes, CNRS-CREGU, Nancy, 86–87.

Dow W. G. (1977): Kerogen studies and geological interpretations. J. Geochem. Explor. 7, 79–99.

Everall N. J., Lumsdon J., Christopher D. J. (1991): The effect of laser-induced heating upon the vibrational Raman spectra of graphites and carbon fibres. Carbon 29, 133–137.

Fiala F. (1970): Silurian and Devonian diabases of the Barrandian. Sbor. geol. Věd, Geol. 17, 7–89 (in Czech).

Frey M., Teichmüller M., Teichmüller R., Mullis J., Künzi B., Breitschmid A., Gruner U., Schwizer B. (1980): Very low-grade metamorphism in external parts of the Central Alps: Illite crystallinity, coal rank and fluid inclusion data. Eclogae Geol. Helv. 73, 173–203.

Galushkin Y. I. (1997): Thermal effects of igneous intrusions on maturity of organic matter: A possible mechanism of intrusion. Org. Geochem. 26, 645–658.

Gentzis T., Freitas T., Goodarzi F., Melchin M., Lenz A. (1996): Thermal maturity of Lower Paleozoic sedimentary successions in Arctic Canada. Amer. Assoc. Petrol. Geol. Bull. 80, 1065–1084.

George S. C. (1992): Effect of igneous intrusion on the organic geochemistry of a siltstone and an oil shale horizon in the Midland Valley of Scotland. Org. Geochem. 18, 705–723.

Goodarzi F. (1990): Graptolite reflectance and thermal maturity of Lower Paleozoic rocks. In: Nuccio V. F., Barker C.E. (eds) Applications of Thermal Maturity Studies to Energy Exploration, 19–22.

Hanson R. B., Barton M. D. (1989): Thermal development of low-pressure metamorphic belts: results from two-dimensional numerical models. J. Geophys. Res. 94 (B8), 10363–10377.

Havlíček V. (1981): Development of a linear sedimentary depression exemplified by the Prague Basin (Ordovician–Middle Devonian; Barrandian area – central Bohemia). Sbor. geol. Věd, Geol. 35, 7–48.

Hillier S., Clayton T. (1989): Illite/smectite diagenesis in Devonian lacustrine mudrocks from northern Scotland and its relationship to organic maturity indicators. Clay Minerals 24, 181–196.

Hoffknecht A. (1991): Mikropetrographische, organisch-geochemische, mikrothermometrische und mineralogische Untersuchungen zur Bestimmung der organischen Reife von Graptolithen-Periderm. Göttinger Arb. Geol. Paläont. 48, 99 p.

Hrabal J. (1989): A study on the reflectance of dispersed organic matter in selected samples of clayey shales of the Barrandian. Geol. hydrometal. uranu 13, 3–17 (in Czech).

Hunt J. M. (1996): Petroleum Geochemistry and Geology, 2nd ed. Freeman Comp., New York.

Ibarra J. V., Muñoz E., Moliner R. (1996): FTIR study of the evolution of coal structure during the coalification process. Org. Geochem. 24, 725–735.

Illich H. H., Grizzle P. L. (1983): Comment on "Comparison of Michigan basin crude oils" by Volger et al. Geochim. Cosmochim. Acta 47, 1151–1155.

Jehlička J., Beny C. (1999): First and second order Raman spectra of naturally highly carbonified organic compounds from metamorphic rocks. J. Molecular Structure 480/481, 541–545.

Junfeng J., Browne P. R. L. (2000): Relationship between illite crystallinity and temperature in active geothermal systems of New Zealand. Clays and Clay Miner. 48, 139–144.

Kosakowski G., Kunert V., Clauser Ch., Franke W., Neugebauer H. J. (1999): Hydrothermal transients in Variscan crust: paleo-temperature mapping and hydrothermal models. Tectonophysics 306, 325–344.

Kříbek B. (1989): Uhlíkaté formace a jejich úloha v metalogenezi Českého masivu [Carbonaceous formations and their role in the metallogeny of the Bohemian Massif]. Doctoral disseration, Charles Univ. Prague (in Czech).

Kříbek B., Hrabal J., Landais P., Hladíková J. (1994): The association of poorly ordered graphite, coke and bitumens in greenschits facies rocks of the Poniklá Group, Lugicum, Czech Republic: the result of graphitization of various types of carbonaceous matter. J. Metamorphic Geol. 12, 493–503.

Krynauw J. R., Behr H. J., Van Den Kerkhof A. M. (1994): Sill emplacement in wet sediments: fluid inclusion and cathodoluminescence studies at Crunehoga, western Drowning Maud Land, Antarctica. J. Geol. Soc. London 151, 777–794.

Le Maitre R.W. (1985): A proposal by the IUGS Subcommission on the systematics of igneous rocks for a chemical classification of volcanites based on the total alkali-silica (TAS) diagram. Aust. J. Earth Sci. 31, 243–255.

Lespade P., Al-Jishi R., Dresselhaus M. S. (1982): Model for Raman scattering from incompletely graphitized carbons. Carbon 20, 427–431.

Lespade P., Marchand A., Couzi M., Cruege F. (1984): Caractérisation de matériaux carbonés par microspectrometrie Raman. Carbon 22, 375–382.

Lin R., Ritz G. P. (1993): Reflectance FT-IR microspectrometry of fossil algae contained in organic-rich shales. Appl. Spectroscopy 47, 265–271.

Mackenzie A. S. (1984): Application of biological markers in petroleum geochemistry. In: Brooks J., Welte D. H. (eds) Advances in Petroleum Organic Geochemistry. Academic Press, London, 115–214.

Malán O. (1980): Petrological investigation of dispersed organic matter (MOD) in the deep bore Tobolka-1. Folia Mus. Rerum Nat. Bohem. Occident., C (Plzeň), 3–51.

Merriman R. J., Frey M. (1999): Patterns of very low-grade metamorphism in metapelitic rocks. In: Frey M., Robinson D. (eds) Low-Grade Metamorphism. Blackwell Science Publ., London, 61–107.

Mullis J., Rahn M., De Capitani C., Stern W. B., Frey M. (1995): How useful is illite "crystallinity" as a geothermometer? Terra Abstracts, Abstract Supplement to Terra Nova 7, 128–129.

Olsson I. (1999): Regional burial vs. local magmatic heat influence of the Rostanga area, Scania, southern Sweden. Geologiska Foereningens I Stockholm. Forerhandlingar (GFF) 121, 209–214.

Perregaard J., Schiener E. J. (1979): Thermal alteration of sedimentary organic matter by a basalt intrusive (Kimmeridgian Shales, Milne Land, East Greenland). Chem. Geol. 26, 331–343.

Peters K. E., Whelan J. K., Hunt J. M., Tarafa H. F. (1983): Programmed pyrolysis of organic matter from thermally altered Cretaceous black shales. Amer. Assoc. Petrol. Geol. Bull. 67, 2137–2149.

Powell T. G., McKirdy D. M. (1973): The effect of source material, rock type and diagenesis on the *n*-alkane content of sediments. Geochim. Cosmochim. Acta 37, 523–633.

Rangin C., Desprairies A., Fontes J. C., Jehanno C., Vernhet S. (1983): Metamorphic processes in sediments in contact with young oceanic crust – East Pacific rise, leg 65. In: Lewis B.R.T., Robinson P. (eds) Init. Rep. Deep Sea Drilling Project 65, 375–389.

Raymond A. C., Murchison D. G. (1988): Development of organic maturation in the aureoles of sills and its relation to sediment compaction. Fuel 67, 1599–1608.

Robert P. (1988): Organic Maturation and Geothermal History. Elf-Aquitane and D. Reidel, Dordrecht.

Roberts S., Tricker M., Marshall J. E. A. (1995): Raman spectroscopy of chitinozoans as a maturation indicator. Org. Geochem. 23, 223–228.

Rouxhet P. G., Robin P. L., Nicaise G. (1980): Characterization of kerogens and of their evolution by infrared spectroscopy. In: Durand B. (ed) Kerogen. Edition Technip, Paris, 163–189.

Saxby J. D., Stephenson L. C. (1987): Effect of igneous intrusion on oil shale at Rundle (Australia). Chem. Geol. 63, 1–16.

Šafanda J., Suchý V., Sýkorová I., Stejskal M., Filip J., Machovič V., Borecká L., Dobeš P. (2003): Thermal history of sedimentary basins of the Czech Republic and its relation to tectonic processes. Acta Montana IRSM AS CR, Ser. AB, 11, 128, 45–54.

Šrámek J. (1978): Relative age of diagenetic carbonate concretions in relation to the sediment porosity. Acta Univ. Carol. Geol., Kratochvíl vol. (1978), 307–321.

Šrámek J., Mráz L. (1984): Chlorite-montmorillonite from the Kosov Quarry near Beroun. In: Konta J. (ed) 9th Conference on Clay Mineralogy and Petrology, Zvolen, 1982, Univerzita Karlova, Praha, 217–231.

Štorch P. (1998): VIII. Volcanism. In: Chlupáč I., Havlíček V., Kříž P., Kukal Z., Štorch P. Palaeozoic of the Barrandian (Cambrian to Devonian), Czech Geological Survey, Prague, 149–164.

Štorch P., Pašava J. (1989): Stratigraphy, chemistry and origin of the Lower Silurian black graptolitic shales of the Prague Basin (Barrandian, Bohemia). Věst. Ústř. Úst. geol. 64, 143–162.

Suchý V., Rozkošný I. (1996): Diagenesis of Clay Minerals and Organic Matter in the Přídolí Formation (Upper Silurian), the Barrandian Basin, Czech Republic: First Systematic Survey. In: Melka K. (ed) XIIIth Conference on Clay Mineralogy and Petrology, Acta Univ. Carol., Geol. 38 (1994), 401–409.

Suchý V., Sýkorová I., Eckhardtová Š., Dobeš P., Stejskal M. (1997): Kontaktní metamorfóza silurských černých břidlic ložní žilou diabasu: studie z lomu Kosov u Berouna, Barrandien [Contact metamorphism of Silurian black shales by a basaltic sill: a case study from the Kosov quarry near Beroun, the Barrandian]. Zpr. geol. Výzk. v Roce 1996, 133–134 (in Czech).

Suchý V., Sýkorová I., Stejskal M., Šafanda J., Machovič V., Novotná M. (2002): Dispersed organic matter from Silurian shales of the Barrandian Basin, Czech Republic: optical properties, chemical composition and thermal maturity. Int. J. Coal Geology 53, 1–25.

Tissot B. P., Welte D. H. (1984): Petroleum Formation and Occurrence, 2nd ed. Springer, Berlin.

Tuinstra F., Koenig J. L. (1970): Raman spectrum of graphite. J. Chem. Phys. 53, 1126–1130.

Underwood M. B., Brocculeri T., Bergfeld D., Howell D. G., Pawlewicz M. (1992): Statistical Comparison Between Illite Crystallinity and Vitrinite Reflectance, Kandik Region of East-Central Alaska. In: Bradley D. C., Dusel-Bacon C. (eds) Geologic Studies in Alaska by the U.S. Geological Survey, 1991; USGS Bulletin 2041, 222–237.

Volk H., Mann U., Burde O., Horsfield B., Suchý V., Wilkes H. (1999): Bitumens, petroleum inclusions and possible source rocks from the Prague Basin (Barrandian, Czech Republic). In: 19th Internat. Meeting on Organic Geochemistry, EAOG, Istanbul 1999, 205–206.

Warr L. N., Rice A. H. N. (1993): Crystallinity Index Standard. Unpublished report (version 1: 29.3. 93), Geologisch-Paläontologisches Institut, Ruprecht-Karls Universität, Heidelberg, 1–46.

Warr L. N., Rice A. H. N. (1994): Interlaboratory standardization and calibration of clay mineral crystallinity and crystallite size data. J. Metamorphic Geol. 12, 141–152.

Wopenka B., Pasteris J. D. (1993): Structural characterization of kerogens to granulite-facies graphite: applicability of Raman microprobe spectroscopy. Amer. Mineral. 78, 533–557.

Yang C., Hesse R. (1991): Clay minerals as indicators of diagenetic and anchimetamorphic grade in an overthust belt, external domain of southern Canadian Appalachians. Clay Minerals 26, 211–231.